Konrad-Zuse-Zentrum
für Informationstechnik Berlin

Takustraße 7
D-14195 Berlin-Dahlem
Germany

PETER WOITKE[1] CHRISTIANE HELLING[1,2]

Formation and structure of quasi-static cloud layers in brown dwarf atmospheres

[1]Zentrum für Astronomie und Astrophysik, TU Berlin, Hardenbergstraße 36, 10623 Berlin
[2]Guest member at ZIB

ZIB-Report 03-11 (Mai 2003)

Formation and structure of quasi-static cloud layers in brown dwarf atmospheres

Peter Woitke Christiane Helling

8. Mai 2003

Abstract

In this paper, first solutions of the dust moment equations developed in (Woitke & Helling 2002) for the description of dust formation and precipitation in brown dwarf and giant gas planet atmospheres are presented. We consider the special case of a static brown dwarf atmosphere, where dust particles continuously nucleate from the gas phase, grow by the accretion of molecules, settle gravitationally and re-evaporate thermally. Applying a kinetic description of the relevant microphysical and chemical processes for TiO_2-grains, the model makes predictions about the large-scale stratification of dust in the atmosphere, the depletion of molecules from the gas phase, the supersaturation of the gas in the atmosphere as well as the mean size and the mass fraction of dust grains as function of depth. Our results suggest that the nucleation occurs in the upper atmosphere where the gas is cool, strongly depleted, but nevertheless highly supersaturated ($S \gg 1$). These particles settle gravitationally and populate the warmer layers below, where the in-situ formation (nucleation) is ineffective or even not possible. During their descent, the particles grow up to radii $\approx 0.3\,\mu\mathrm{m} ... 150\,\mu\mathrm{m}$, depending on the efficiency of convective mixing, thereby consuming the remaining condensable elements from the gas phase and nearly saturating the gas around the cloud base. The particles finally sink into layers which are sufficiently hot to cause their thermal evaporation. Hence, an effective transport mechanism for condensable elements exists in brown dwarfs, which depletes the gas above and enriches the gas below the sublimation temperature (cloud base) of a considered solid/liquid material. In the stationary case studied here, this downward directed element transport by precipitating dust grains is balanced by an upward directed flux of condensable elements from the deep interior of the star via convective mixing (no dust without mixing). We find a self-regulation mechanism which leads to an approximate phase equilibrium ($S \approx 1$) around the cloud base. The mass fraction of dust present in the atmosphere results be to approximately given by the mass fraction of condensable elements in the gas being mixed up.

1 Introduction

For ultra-cool stars and giant gas planets, the classical theory of stellar atmospheres suffers from the lack of a reliable theory for the formation of solid particles and fluid droplets (henceforth called dust) in the atmosphere with are

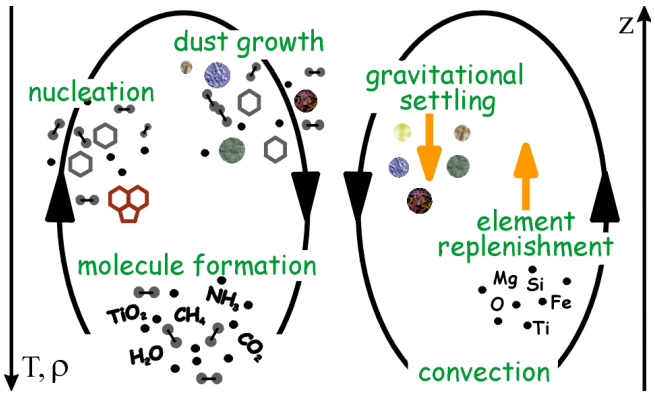

Abbildung 1: Sketch of the convective dust formation in brown dwarf atmospheres: Life cycle of dust grains in sub-stellar objects.

important opacity carriers. A standard method to predict the amount and the size distribution of dust particles of different kinds as function of depth, and their feedback on the abundances in the atmosphere is not yet at hand.

Static model atmosphere calculations for brown dwarfs with frequency-dependent radiative transfer and mixing-length theory (e. g. Allard et al. 2001, Marley et al. 2002, Tsuji 2002) have, therefore, mainly used *ad-hoc assumptions* for the treatment of the dust component so far. Depending on the purpose of the model, the dust is simply disregarded, the dust is assumed to be fully condensed and present or to have rained out completely, leaving behind a saturated, i. e. strongly metal-deficient atmosphere. In each case, the spectral appearance of molecular bands in the calculated spectra and the structure of the atmosphere results to be quite different, which underlines the necessity of a consistent modelling of the dust component in brown dwarf atmospheres.

The formation and precipitation of dust particles has furthermore been suggested to cause the observed evolutionary sequence from L to T dwarfs, which change their $J-K$ colour from red to blue with increasing age (Kirkpatick et al. 1999, Marley et al. 2002, Burgasser et al. 2002). As the brown dwarfs evolve along their cooling trajectory, the active dust forming regions are suggested to sink below the photospheric level due to temperature constraints, which causes the star to emit bluer than at earlier ages, when the effective temperature was higher.

Thus, a strong need exists for a more profound modelling of the dust component in ultra-cool stellar atmospheres. In particular, the dust size distribution has often been treated inattentively in the models so far, e. g. using the distribution function of the interstellar medium (e. g. Allard et al. 2001). Several works have addressed this problem (e. g. Lunine et al. 1989, Ackermann & Marley 2001, Cooper et al. 2003) and have arrived at some first-order solutions. These works are guided by stability considerations and follow a decision tree based on the local time-scale arguments of Rossow (1978), which are originally based on the experience with the earth's atmosphere. However, these works do not aim at a kinetic description of the relevant microphysical and chemical processes responsible for the dust formation, precipitation and evaporation.

Without the replenishment with condensable elements, the final consequence

of the gravitational settling of dust particles in a static atmosphere is a saturated gas without dust. However, the convective mixing counteracts this mechanism. Brown dwarfs are known to be nearly fully convective (Chabrier & Baraffe 1997, Tsuji 2002). Consequently, a non-continuous and spatially inhomogeneous mixing of the upper atmosphere with gas from the deep interior can be expected. The dust formation process is probably triggered by this mixing, especially in upward directed, hot convective gas streams. The dust grains nucleate in such metal-rich, i. e. supersaturated upwinds and rain out as soon as their sizes have become sufficiently large, e. g. via the accretion of molecules. The sinking grains will finally reach deeper atmospheric layers which are hot enough to cause their thermal evaporation, which completes the life cycle of a dust grain in a brown dwarf atmosphere (see Fig. 1). Since the vertical extension of a brown dwarf atmosphere is quite small – typical density scale heights are as small as $H_p \approx 10^6\,\mathrm{cm}$ – all these processes occur in a thin layer, similar to the weather in the Earth's atmosphere. Comparable weather-like features can be observed in giant gas planets, e. g. the vivid fluid motion on Jupiter's surface (e. g. Vasavada et al. 1998, Gierasch et al. 2000, Gelino & Marley 2000).

In Woitke & Helling (2002, hereafter Paper II), a time-dependent physical description of the dust component in brown dwarf atmospheres has been developed by extending the classical dust moment method developed by Gail & Sedlmayr (1988), Gauger et al. (1990) and Dominik et al. (1993) to include size-dependent particle drift. Two different systems of partial differential equations in conservation form have been derived for the two relevant limiting cases of small Knudsen numbers (subsonic free molecular flow) and large Knudsen numbers (laminar flow). These equations offer a unique method to simultaneously model nucleation, growth, evaporation, element consumption and gravitational settling of heterogeneous grains in time-dependent sub-stellar atmospheres.

In this paper, we aim at a first application of this method in the frame of a homogeneously mixed static atmosphere, where we are mainly interested in the basic control mechanisms responsible for the formation and the structure of a quasi-static cloud layer. As example for refractory grains, we solve the dust moment equations for TiO_2-grains for the special case of a prescribed plane-parallel atmospheric gas stratification, where dust particles continuously form, settle gravitationally and evaporate, i. e. we assume the dust component to be stationary. We summarise the extended dust moment equations and derive their special form for the plane-parallel, static, stationary case in Sect. 2, along with a short description of the applied boundary and closure conditions, and our numerical method to solve the resulting system of ordinary differential equations. In Sect. 3, the calculated vertical structures of quasi-static cloud layers in brown dwarf atmospheres are presented. We discuss these results with respect to previous works in Sect. 4. Our conclusions are outlined in Sect. 5.

2 The model of a quasi-static cloud layer

In the following, we apply the kinetic description for nucleation, growth, evaporation, and gravitational settling of dust grains as developed in Paper II to a quasi-static brown dwarf atmosphere. We consider the subsonic, large Knudsen number case (lKn = $\{\mathrm{Kn} \gg 1$ and $|\vec{v}_{\mathrm{dr}}| \ll c_{\mathrm{T}}\}$, compare Paper II), because – as the results will show – the majority of dust grains building up the cloud layer

fall into this regime[1]. For this special case, the following system of dust moment equations has been derived in Paper II:

$$\frac{\partial}{\partial t}\left(\rho L_j\right) + \nabla\cdot\left(\vec{v}_{\rm gas}\,\rho L_j\right) = \\ = V_\ell^{j/3} J(V_\ell) + \frac{j}{3}\,\chi_{\rm lKn}^{\rm net}\,\rho L_{\rm j-1} - \xi_{\rm lKn}\nabla\left(\frac{L_{j+1}}{c_T}\,\vec{e}_r\right) \quad (1)$$

$$\text{with} \quad \chi_{\rm lKn}^{\rm net} = \sqrt[3]{36\pi}\sum_{r=1}^{R}\Delta V_r\,n_r\,v_r^{\rm rel}\alpha_r\left(1-\frac{1}{S_r}\right) \quad (2)$$

$$\xi_{\rm lKn} = \frac{\sqrt{\pi}}{2}\left(\frac{3}{4\pi}\right)^{1/3} g\rho_{\rm d}\,. \quad (3)$$

$L_j = \int_{V_\ell}^{\infty} f(V)V^{j/3}\,dV$ [cm^j g^{-1}] ($j = 0, 1, 2, ...$) is the $j^{\rm th}$ moment of the grain size distribution function in volume space $f(V)$ [cm^{-6}], $\chi_{\rm lKn}^{\rm net}$ [cm/s] is the net growth speed, $\xi_{\rm lKn}$ [dyn cm^{-3}] the drag force density, n_r [cm^{-3}] the particle density of the key species of surface reaction r in the gas phase and S_r its generalised supersaturation ratio. For more details about Eqs. (1–3) please consult Paper II.

The element depletion is taken into account by evaluating the consumption of each involved element i with relative abundance to hydrogen ϵ_i by nucleation and growth

$$\frac{\partial}{\partial t}\left(n_{\langle\rm H\rangle}\epsilon_i\right) + \nabla\cdot\left(\vec{v}_{\rm gas}\,n_{\langle\rm H\rangle}\epsilon_i\right) = -\nu_{i,0}\,N_\ell\,J(V_\ell) \\ - \sqrt[3]{36\pi}\,\rho L_2\sum_{r=1}^{R}\nu_{i,r}\,n_r v_r^{\rm rel}\alpha_r\left(1-\frac{1}{S_r}\right) \quad (4)$$

with stoichiometric ratios of homogeneous nucleation $\nu_{i,0}$ and surface reactions $\nu_{i,r}$. $n_{\langle\rm H\rangle}$ is the total hydrogen nuclei density ($\rho = 1.427\,{\rm amu}\,n_{\langle\rm H\rangle}$ for solar abundances).

2.1 Application to TiO_2

Only one example dust species will be considered in the following, i. e. we assume the dust grains to be composed of a unique solid material. The following complications would arise if different kinds of condensates were considered simultaneously: (i) Dust grains of different kinds may condensate independently, competing for the remaining condensable elements in the gas phase. (ii) One solid species may provide the seed particles for another solid species to condense at its surface *(core-mantle grains)*. (iii) Two or more solid species may condense simultaneously on the same surface to form *dirty grains*. These details, which would considerably complicate the understanding of the basic control mechanisms, are disregarded here, but will be addressed in a future paper[2].

[1] Small Knudsen numbers may occur in the innermost layers around the cloud base, where the gas densities are highest and the dust grains are largest (see Sect. 4.1). According to the purpose of this paper, we will nevertheless avoid at first the troublesome Knudsen number fall differentiation as discussed in Paper II.

[2] Eqs. (1–3) are formulated for dirty grains, i. e. it is possible to discuss these questions by means of these equations.

As exemplary solid species, typical for refractory grains, we choose *rutile* TiO_2[s] because (i) it is among the thermodynamically most stable solid materials known and (ii) the monomer (the TiO_2 molecule) is abundant in the gas phase according to chemical equilibrium (e. g. Allard et al. 2001). Therefore, the formation of TiO_2 seed particles from the gas phase can be assumed to proceed via a simple stepwise addition of TiO_2 molecules to $(TiO_2)_N$ clusters *(homogeneous nucleation)* which enables us to apply classical nucleation theory in order to calculate the nucleation rate $J_\star$. In contrast, other high temperature condensates like corundum (Al_2O_3[s]) often have no stable monomer in the gas phase (Patzer et al. 1998) and the nucleation of such species seems questionable since three or more body collisions would be required to form small clusters of that kind in the gas phase. It seems more likely, that the condensation of materials like Al_2O_3 already requires the existence of some surface, i. e. the presence of seed particles provided by homogeneously nucleating species, as for example TiO_2.

For the growth and evaporation of macroscopic rutile dust particles the following two chemical surface reactions are considered

$$\begin{aligned} TiO_2 + (TiO_2[s])_N &\rightleftharpoons (TiO_2[s])_{N+1} && (r=1) \\ TiO + H_2O + (TiO_2[s])_N &\rightleftharpoons (TiO_2[s])_{N+1} + H_2 && (r=2). \end{aligned}$$

Because of the small titanium abundance, the rate of reaction $r=2$ is limited by the TiO number density in the gas phase and hence its key species is identified as $n_2 = n_{TiO}$. Clearly for reaction $r=1$, the key species is $n_1 = n_{TiO_2}$. Since both reactions transform one unit of the solid material, we put $\Delta V_1 = \Delta V_2 = \Delta V_{TiO_2}$ and $S_1 = S_2 = S_{TiO_2}$ (see Paper II). Furthermore, we have $R = 2$, $i = 1$ for titanium and $i = 2$ for oxygen, $\nu_{1,0} = \nu_{1,1} = \nu_{1,2} = 1$ and $\nu_{2,0} = \nu_{2,1} = \nu_{2,2} = 2$. Further data required to calculate $J_\star$, $\chi^{\rm net}_{\rm lKn}$ and $\xi_{\rm lKn}$ are listed in Sect. 2.6.

2.2 Treatment of convective mixing

As shown in Appendix A, the coupled system of dust moment equations (1) and element consumption equations (4) has no other than the trivial solution $L_j = 0$ in the static stationary case, where all l.h.s. terms vanish. It is also shown in Appendix A that the atmosphere cannot be supersaturated anywhere in the atmosphere $S_r \leq 1$ in this case. The physical interpretation of this solution is that dust grains have once formed in the sufficiently cool layers, have consumed all available condensable elements up to the saturation level, and have finally left the model volume by gravitational settling. Consequently, a truly static atmosphere must be dust-free which – in this generality – contradicts the observations.

This picture changes, however, if we take into account a continuous or sporadic mixing of the atmosphere with gas from deeper layers as expected to be caused by the convection. This mixing leads to a replenishment of the gas with fresh, uncondensed matter from the deep interior of the brown dwarf. Adopting the most simple case of a continuous, uniform mixing with uncondensed gas of

solar abundances, Eqs. (1) and (4) are extended as

$$\frac{\partial}{\partial t}\left(\rho L_j\right) + \nabla\left(\vec{v}_{\rm gas}\,\rho L_j\right) \;=\; -\frac{\rho L_j}{\tau_{\rm mix}} + V_\ell{}^{j/3} J_\star \;+\; \frac{j}{3}\,\chi^{\rm net}_{\rm lKn}\rho L_{j-1} \;+\; \xi_{\rm lKn}\,\nabla\left(\frac{L_{j+1}}{c_T}\,\vec{e}_r\right) \quad (5)$$

$$\frac{\partial}{\partial t}\left(n_{\langle \rm H\rangle}\epsilon_i\right) + \nabla\left(\vec{v}_{\rm gas}\,n_{\langle \rm H\rangle}\epsilon_i\right) \;=\; \frac{n_{\langle \rm H\rangle}\left(\epsilon_i^0 - \epsilon_i\right)}{\tau_{\rm mix}} - \nu_{i,0} N_\ell J_\star - \sqrt[3]{36\pi}\,\rho L_2 \sum_{r=1}^{R} \nu_{i,r} n_r v_r^{\rm rel} \alpha_r \left(1 - \frac{1}{S_r}\right). \quad (6)$$

$\tau_{\rm mix}$ is a characteristic mixing time-scale, which is treated here as a free parameter. We thereby assume that the gas/dust mixture is continuously replaced by dust-free gas of solar abundances in all layers on a constant time-scale $\tau_{\rm mix}$. ϵ_i is the actual abundance of element i in the gas phase and ϵ_i^0 its solar value (Anders & Grevesse 1989).

In Eqs. (5) and (6), we have replaced $J(V_\ell)$ by the nucleation rate $J_\star$. While both terms are in fact nearly equal in a supersaturated gas $S>1$ (Gail & Sedlmayr 1988), this is an approximation in the undersaturated case, where all particles evaporate. Here, $J(V_\ell) = f(V_\ell)\frac{dV}{dt}\big|_{V=V_\ell}$ should be calculated from the actual cluster size distribution function at the lower boundary $f(V_\ell)$ and its volume decrement $\frac{dV}{dt}\big|_{V=V_\ell} < 0$. Unfortunately, $f(V_\ell)$ is not known[3], so we use $J(V_\ell) = J_\star$ as a simplifying approximation which underestimates the influence of evaporation on the dust moments. However, as the results will show, the gravitationally settling dust grains evaporate very quickly, which affects only a thin layer below the cloud base.

In the following, we assume a quasi-static atmosphere ($\vec{v}_{\rm gas} = 0$), plane-parallel geometry ($\vec{e}_r = \vec{e}_z$), constant gravity ($g = \rm const$) and a stationary dust component ($\frac{\partial L_j}{\partial t} = 0$). In this special case, the system of moment equations (5) for $j = 0, 1, 2$ degenerates into the following system of ordinary differential equations:

$$\begin{aligned} -\frac{d}{dz}\left(\frac{L_1}{c_T}\right) &= \frac{1}{\xi_{\rm lKn}}\left(-\frac{\rho L_0}{\tau_{\rm mix}} + J_\star\right) \\ -\frac{d}{dz}\left(\frac{L_2}{c_T}\right) &= \frac{1}{\xi_{\rm lKn}}\left(-\frac{\rho L_1}{\tau_{\rm mix}} + V_\ell{}^{1/3} J_\star + \frac{1}{3}\chi^{\rm net}_{\rm lKn}\,\rho L_0\right) \\ -\frac{d}{dz}\left(\frac{L_3}{c_T}\right) &= \frac{1}{\xi_{\rm lKn}}\left(-\frac{\rho L_2}{\tau_{\rm mix}} + V_\ell{}^{2/3} J_\star + \frac{2}{3}\chi^{\rm net}_{\rm lKn}\,\rho L_1\right). \end{aligned} \quad (7)$$

[3]The numerical scheme proposed by Gauger et al. (1990) to reconstruct the size distribution function from the history of $J_\star$ and $\chi^{\rm net}_{\rm lKn}$ in each gas element, cannot be applied here, since position coupling is not valid.

2.3 Auxiliary condition

In the static and stationary case, the element consumption equation (Eq. 6) becomes an algebraic auxiliary condition for each element i

$$\frac{n_{\langle \mathrm{H} \rangle}(\epsilon_i^0 - \epsilon_i)}{\tau_{\mathrm{mix}}} = \nu_{i,0} N_\ell J_\star + \sqrt[3]{36\pi}\,\rho L_2 \sum_{r=1}^{R} \nu_{i,r} n_r v_r^{\mathrm{rel}} \alpha_r \left(1 - \frac{1}{S_r}\right) , \quad (8)$$

which is coupled to the gas phase chemistry, the supersaturation ratio and the nucleation rate, and depends on the total surface area of the dust component ($\propto \rho L_2$). In our example, two equations have to be solved for $i = 1$ (titanium) and $i = 2$ (oxygen).

Technically speaking, the system of non-linear algebraic equations (8) is solved by iteration in each layer z prior to the evaluation of the r.h.s. terms of the differential equations (7). Given the density and temperature of the gas, $n_{\langle \mathrm{H} \rangle}(z)$ and $T(z)$, and an estimate of the unknowns $\epsilon_i'(z)$, all particle densities $n_k(z)$ (atoms, electrons, ions and molecules) are calculated in chemical equilibrium. Elements other than Ti and O are assumed to have solar abundances. We use 14 elements (H, He, C, N, O, Si, Mg, Al, Fe, S, Na, K, Ti, Ca) and 155 molecules in our chemical equilibrium code with equilibrium constants fitted to the thermodynamical molecular data from the electronic version of the JANAF tables (Chase et al. 1985). First ionisation states of all elements are sufficient to calculate reliable molecular concentrations also at higher temperatures (see discussion in Helling et al. 2000). From these particle densities, the supersaturation ratio $S_{\mathrm{TiO_2}}(z)$ and the nucleation rate $J_\star(z)$ are calculated, and the remaining errors in the auxiliary conditions (Eqs. 8) are quantified. A Newton-Raphson iteration is finally applied to find the root $\epsilon_i(z)$ of Eqs. (8).

2.4 Closure condition

The system of moment Eqs. (7) is not closed, since L_0 appears on the r.h.s., whereas the equations are solved for L_j ($j = 1, 2, 3, ...$) only. A solution of such an open moment system is only possible if a physically reasonable and numerically stable closure condition in the form $\mathcal{F}(L_0, L_1, L_2, L_3, ...) = 0$ can be provided. For numerical reasons, this closure conditions should be fast, e. g. preferably analytical and invertible concerning L_0.

We have tested seven different approaches for this closure condition, including the scheme of (Deuflhard & Wulkow 1989, Wulkow 1992) in application to different weight functions $\Psi^\alpha(V)$ (see Paper II). In general, the solutions obtained with different approaches are quite similar, but the convergence of the model may fail for certain choices of the closure condition, in particular regarding the undersaturated layers below the cloud base. In the following, we only describe a very simple but stable scheme, which is based on the experience that the dust moments can reasonably well be approximated by a power-law as function of the index j in most cases,

$$y(j) = \alpha\, j^{\,\beta} \qquad \text{with} \qquad y(j) = \frac{L_j}{L_{j-1}} . \quad (9)$$

Given the moments L_j for $j \in \{1,2,3\}$, the coefficient α and the exponent β can be expressed by

$$\alpha = \frac{L_2}{L_1\, 2^\beta} \qquad \text{and} \qquad \beta = \frac{\log\left(L_1 L_3 / L_2^2\right)}{\log(3/2)} \;, \tag{10}$$

and the desired equation for the 0^{th} dust moment reads

$$L_0 = \frac{L_1}{\alpha} \;. \tag{11}$$

This closure condition has proven to be most successful.

2.5 Boundary condition

The negative sign on the l.h.s. of Eqs. (7) suggests an inward rather than an outward integration, naturally tracing the drift motion of the grains. We therefore integrate Eqs. (7) *inward*, starting from an outer boundary $z_{\max}$, for which boundary conditions must be supplied. We arbitrarily choose

$$L_j(z = z_{\max}) = 0 \;, \tag{12}$$

i. e. we assume the atmosphere to be dust-free at the outer boundary. The numerical solutions are found to be only marginally affected by the choice and position of the outer boundary, as long as it is located well above (typically 10 scale heights above) the $P = 1\,\text{bar}$ level. At these high altitudes, the importance of the derivative terms in Eqs. (7) is small and the solution is mostly determined by the auxiliary conditions (Eqs. 8), where the boundary condition does not enter. The dust moments are observed to relax quickly toward particular values, independent of the chosen boundary condition.

2.6 Material quantities

The homogeneous nucleation rate $J_\star$ of $(\text{TiO}_2)_N$ clusters is calculated by applying modified classical nucleation theory according to the scheme of Gail et al. (1984) with parameters $\sigma^{\text{TiO}_2} = 620\,\text{erg/cm}^2$ and $N_f^{\text{TiO}_2} = 0$. These parameters, including the "surface tension" σ, result from a fit to quantum mechanical *ab-initio* calculations (density functional theory) for *small* TiO_2 clusters (Jeong 2000) and hence do not represent the bulk phase.

The following data completes the problem. The monomer volume $\Delta V_{\text{TiO}_2} = 3.135 \cdot 10^{-23}\,\text{cm}^{-3}$ results from the rutile density $\rho_{\text{d}} = 4.23\,\text{g cm}^{-3}$ and its monomer weight $m_{\text{TiO}_2} = 79.90\,\text{amu}$. $\alpha_r = 1$ and $N_\ell = 1000$ are assumed. The saturation vapour pressure $p^{\text{vap}}_{TiO_2}(T)$ has been fitted to the JANAF-tables (1985, electronic version) such that the supersaturation ratio of rutile can be expressed by

$$S^{\text{TiO}_2} = \frac{n_{\text{TiO}_2} kT}{\exp(35.8027 - 74734.7/T)[\text{dyn/cm}^2]} \;. \tag{13}$$

2.7 Prescribed atmospheric structure

As underlying atmospheric gas stratification, $n_{\langle \mathrm{H} \rangle}(z)$ and $T(z)$, we adopt two model structures for brown dwarf atmospheres with $\log g = 5$ and two different values of the effective temperature $T_{\mathrm{eff}} = 1400\,\mathrm{K}$ and $T_{\mathrm{eff}} = 1000\,\mathrm{K}$, respectively, kindly provided by T. Tsuji (2002). These reference models are calculated via the standard assumptions of classical stellar atmospheres (hydrostatic equilibrium, frequency-dependent radiative transfer, mixing length theory, microturbulence broadening). We adopt his "case A"-models, where dust formation is ignored. For models which include Fe, Al_2O_3 and $MgSiO_3$ as dust species in different simplified ways ("case B" and "case C") we refer to Tsuji (2002). At this point, we want to clarify, that the underlying atmospheric structure $n_{\langle \mathrm{H} \rangle}(z)$ and $T(z)$ is *prescribed*. Although obviously relevant, the properties of the calculated TiO_2 dust particles have technically no influence on the atmospheric structure in this paper. Indeed, a consistent treatment of atmosphere and cloud structure would be advisable, which in fact seems possible and straightforward by simultaneously solving the equations for hydrostatic equilibrium, radiative transfer, convection and dust-chemistry.

2.8 Numerical method

Equation (7) is a system of ordinary differential equations of first order which can be solved by standard numerical methods. The differential equations are integrated inward by means of the variable transformation $z' = z_{\mathrm{max}} - z$ using the RADAU 5 – solver for stiff ordinary differential equations (Hairer & Wanner 1991). For test purposes, the equation of hydrostatic equilibrium $dP_{\mathrm{gas}}/dz = -\rho g$ is solved in addition to the three moment equations (7), where the actual gas pressure $P = \sum_i n_i kT$ results from the chemical equilibrium calculations. The integration is stopped as soon as one of the dust moments becomes negative, indicating that the dust has completely evaporated.

3 Results

The calculated cloud structures in an atmosphere with $\log g = 5$ and $T_{\mathrm{eff}} = 1400\,\mathrm{K}$ are depicted in Figs. 2 and 3, considering a sequence of decreasing values for the mixing time-scale ($\tau_{\mathrm{mix}} = 10^6\,\mathrm{s} \ldots 10^3\,\mathrm{s}$). The 1st panels show the underlying static model structure (always identical) and panels 2–5 depict the calculated dust and gas properties which result from the consistent solution of the dust moment and element conservation equations.

Before we discuss these structures in detail, some general features of the model calculations are described first. The base of the TiO_2 cloud layer (here defined by $S = 1$ or $\chi^{\mathrm{net}}_{\mathrm{lKn}} = 0$) is found to be located at $P \approx 9.0\,\mathrm{bar}$ ($T \approx 1960\,\mathrm{K}$) in the $T_{\mathrm{eff}} = 1400\,\mathrm{K}$ models, independent of the value assumed for the mixing time-scale τ_{mix}. The cloud stretches up high into the atmosphere with an almost constant dust-to-gas ratio ($\propto \epsilon^{\mathrm{dust}}_{\mathrm{Ti}}$, see 3rd panel) which is approximately given by a fully condensed solar composition gas ($\epsilon^{\mathrm{dust}}_{\mathrm{Ti}} \lesssim \epsilon^{0}_{\mathrm{Ti}}$)[4]. In contrast, the amount of Ti left in the gas phase $\epsilon^{\mathrm{gas}}_{\mathrm{Ti}}$ depends strongly on the altitude above

[4]This result, however, depends on the assumptions concerning the convective mixing, as discussed in Sect. 3.4 and 4.2.

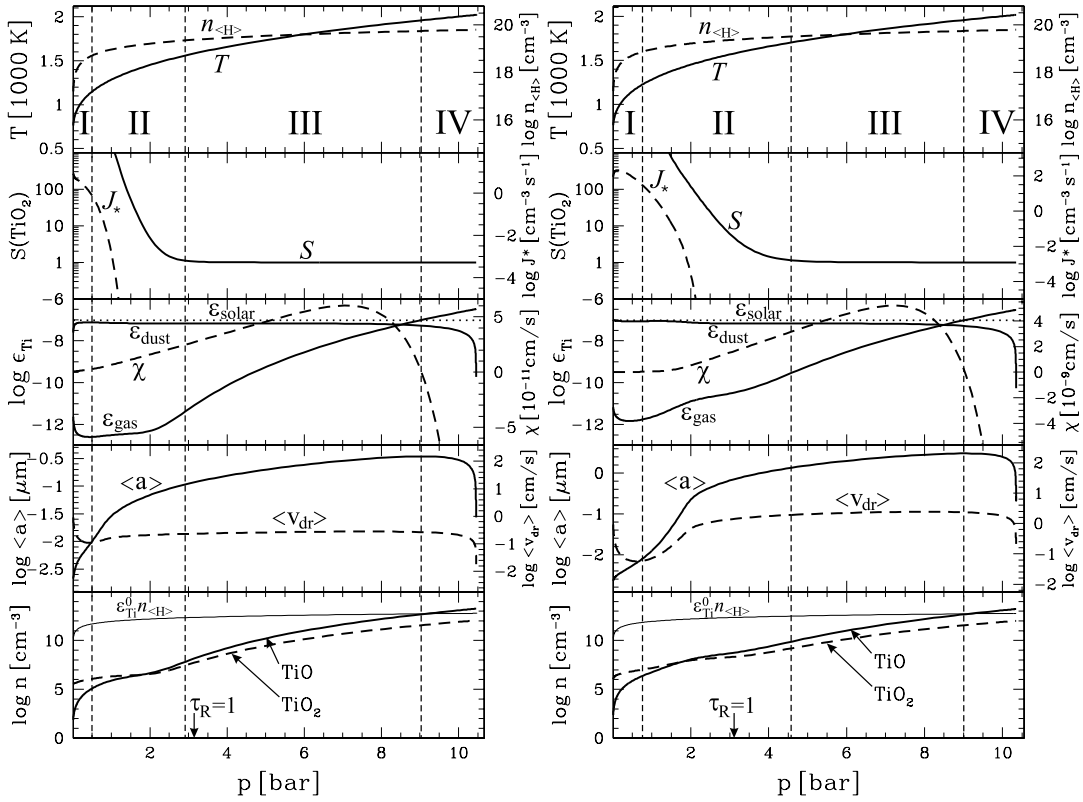

Abbildung 2: Calculated structures of the TiO_2 cloud layer for different mixing time-scales $\tau_{\rm mix}$ (**l.h.s.:** 10^6 s – **r.h.s.:** 10^5 s) in a brown dwarf atmosphere with $T_{\rm eff}$=1400K and $\log\, g = 5$. **1st panel:** prescribed gas temperature T (solid) and total hydrogen nuclei density $n_{\langle \rm H \rangle}$ (dashed), according to the model of Tsuji (2002). **2nd panel:** supersaturation ratio $S^{\rm TiO_2}$ (solid) and nucleation rate $J_\star$ (dashed). **3rd panel:** Ti abundance in the dust phase $\epsilon^{\rm Ti}_{\rm dust} = \rho L_3 / (n_{\langle \rm H \rangle} \Delta V_{\rm TiO_2})$ and in the gas phase $\epsilon^{\rm Ti}_{\rm gas}$. The solar value $\epsilon_{\rm solar} = \epsilon^0_{\rm Ti}$ is additionally indicated by a thin straight line. The dashed line shows the growth velocity $\chi^{\rm net}_{\rm lKn}$. **4th panel:** mean particle size $\langle a \rangle = \sqrt[3]{3/(4\pi)}\, L_1/L_0$ (solid) and mean drift velocity $\langle v_{\rm dr} \rangle = \sqrt{\pi} g \rho_{\rm d} \langle a \rangle \,/\, (2 \rho c_T)$ (dashed, see Eq. (66) in Paper II). **5th panel:** molecular particle densities of TiO (solid) and TiO_2 (dashed). For comparison, the hypothetical total titanium nuclei density for solar abundances $n_{\langle \rm H \rangle} \epsilon^0_{\rm Ti}$ is depicted by the thin solid line.

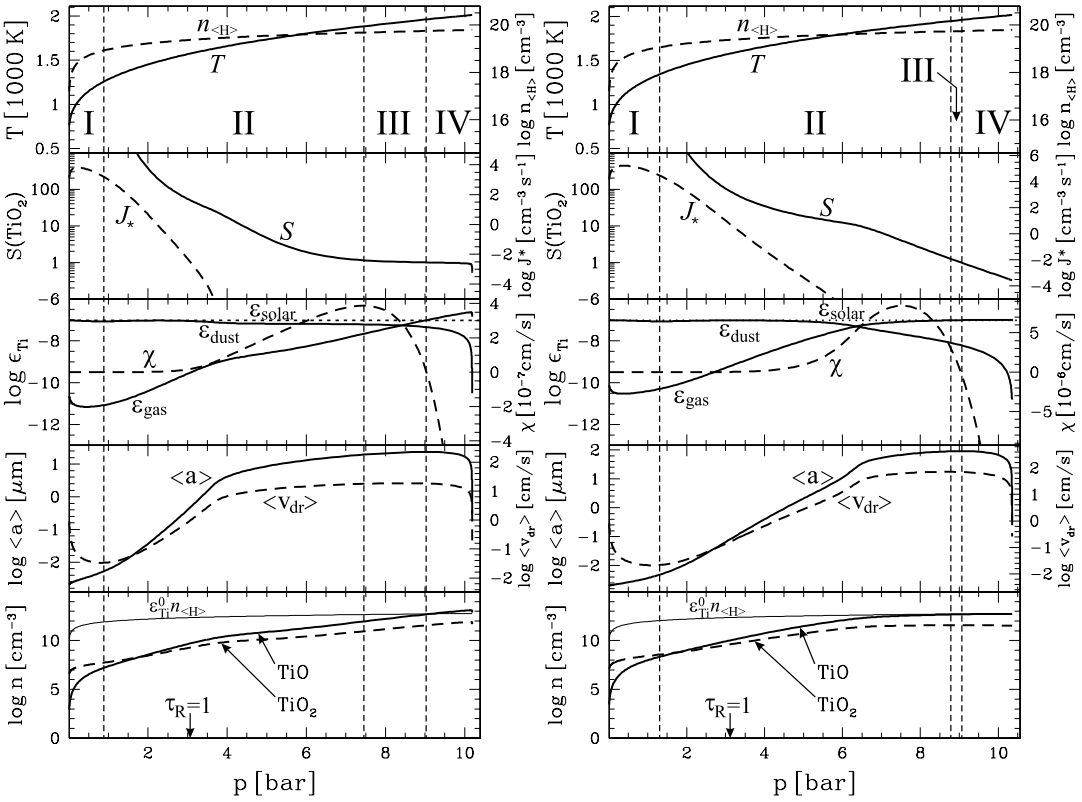

Abbildung 3: Same like Fig. 2, but for $\tau_{\rm mix} = 10^4$ s (l.h.s.) and $\tau_{\rm mix} = 10^3$ s (r.h.s.).

the cloud base. The gas becomes more and more depleted (metal-poor) in the higher atmospheric layers. Interestingly, the cloud layer also stretches well below its base (down to $P \approx 10$ bar with a geometrical distance to the cloud base of ≈ 100 m in this model)[5], where the undersaturated gas is populated by evaporating grains which rain in from above.

3.1 Structure of a quasi-static cloud layer

The vertical structure of the cloud layers results from a competition between the four relevant physical processes: mixing, nucleation, growth/evaporation and drift. Following the cloud structures inward (from the left to the right e. g. in the l.h.s. plot of Fig. 3) roughly four different regions can be distinguished, which are characterised by different dominating processes concerning the dust component, consistent with the classification outlined in Paper II. The spatial extensions of these regions marked by I to IV depend on $\tau_{\rm mix}$ and the stellar parameters.

I. Region of efficient nucleation: Nucleation takes place mainly in the upper parts of the atmosphere, where the temperatures are low and the densities are small but not too small[4]. Although the gas is strongly depleted in heavy elements in these layers ($\epsilon_{\rm Ti} \approx 10^{-5.5} \epsilon^0_{\rm Ti}$ for $\tau_{\rm mix} = 10^6$ s; $\epsilon_{\rm Ti} \approx 10^{-3.5} \epsilon^0_{\rm Ti}$ for

[5]The size of this region may be overestimated because of the $J(V_\ell) \approx J_\star$ approximation, see Sect. 2.2.

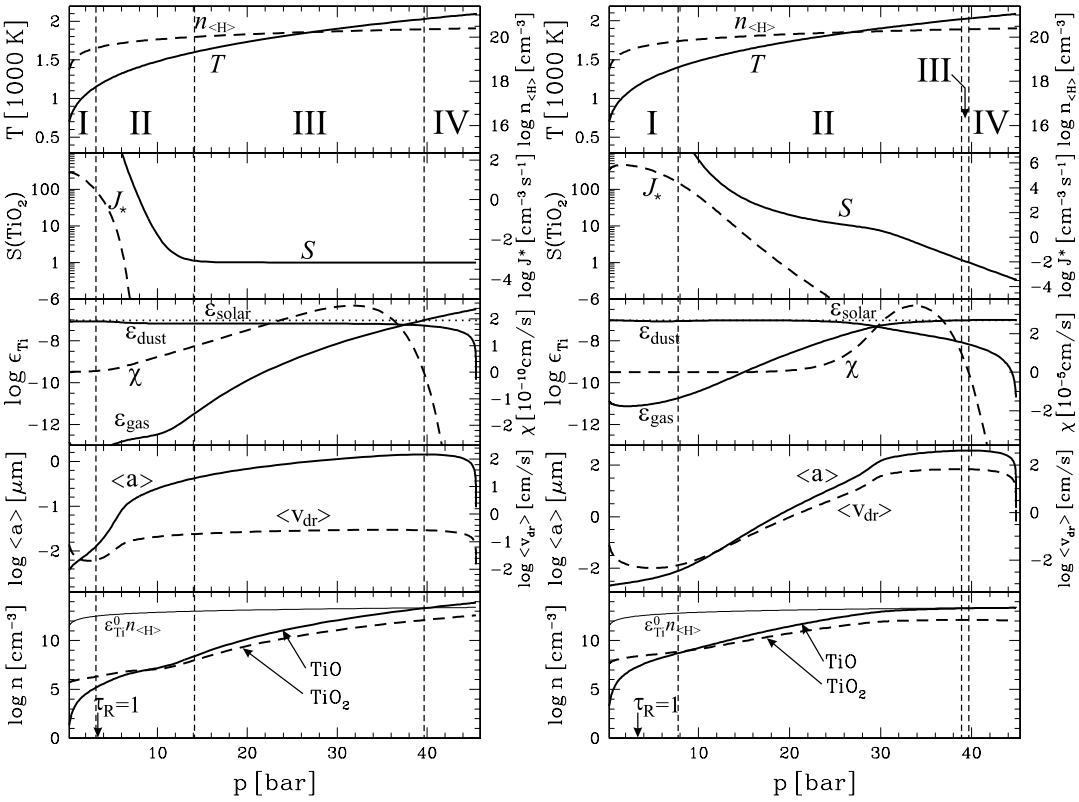

Abbildung 4: Same like Fig. 2, but for effective temperature $T_{\rm eff} = 1000$ K (**l.h.s.:** $\tau_{\rm mix} = 10^6$ s — **r.h.s.:** $\tau_{\rm mix} = 10^3$ s).

$\tau_{\rm mix} = 10^3$ s, see 3$^{\rm rd}$ panel), it is nevertheless highly supersaturated ($S > 1000$) such that homogeneous nucleation takes place efficiently. The important physical processes are here mixing $\leftrightarrow$ nucleation, i. e. the condensable elements mixed up into the upper atmosphere almost instantaneously nucleate, forming the first seed particles[6]. Since very much seed particles are produced in this way, the resulting dust grains remain very small in this region $\langle a \rangle < 0.01\,\mu$m (which in fact corresponds to the parameter N_ℓ describing the minimum size of clusters regarded as "dust") and have a very small mean drift velocity $\langle v_{\rm dr} \rangle \lesssim 0.1 \ldots 1\,$mm/s.

II. Dust growth region: With the inward increasing temperature, the supersaturation ratio S decreases exponentially which leads to a drastic decrease of the nucleation rate $J_\star$. Consequently, nucleation becomes unimportant at some point, i. e. *the in-situ formation of dust grains becomes impossible in region II.* The important physical processes are here mixing $\leftrightarrow$ growth, i. e. the condensable elements mixed up by convection mainly condense on the surfaces of already existing particles, which have been created in region I and have moved into region II by drift. The gas is still strongly supersaturated $S \gg 1$,

[6] To our surprise, the details of the applied nucleation theory have almost no effect on the resulting cloud structures. We have calculated test models with an arbitrarily modified value of the surface tension $\sigma^{\rm TiO_2} = 500\,{\rm erg/cm^2}$, which did not result in any noticeable changes. An explanation can be found via Eq. (8): As long as the total surface area of the dust particles ($\propto \rho L_2$) is negligible, the nucleation rate must equal $J_\star \approx n_{\langle {\rm H} \rangle}\, \epsilon_i^0 / (\nu_{i,0}\, N_\ell\, \tau_{\rm mix})$, provided that $\epsilon_i \ll \epsilon_i^0$. Consequently, a change of $\sigma^{\rm TiO_2}$ results in a change of $\epsilon_{\rm Ti}$, but does not affect $J_\star$ significantly.

indicating that the growth process remains incomplete, i. e. the condensable elements being mixed up are not exhaustively consumed by dust growth. The dust component in region II is characterised by an almost maximum (solar) dust/gas ratio $\epsilon_{\rm Ti}^{\rm dust} \lesssim \epsilon_{\rm Ti}^{0}$, while the mean particle size and the mean drift velocity increase inward. Since the total dust volume per gas mass ($\propto L_3$) is nearly constant and $\langle a \rangle$ increases, the total number of grains per gas mass ($\propto L_0$) and their total surface ($\propto L_2$) decrease.

III. Saturated rain: As the gas density increases inward, the growth becomes finally more efficient than the mixing. Thus, the growth process becomes almost complete which results in a nearly saturated gas $S \gtrsim 1$. Region III is therefore characterised by *a self-regulation mechanism* which leads to an approximate phase equilibrium above the cloud base. The important physical processes are mixing $\leftrightarrow$ drift, i. e. the gain of dust volume by growth (excess of condensable elements provided by the mixing) is balanced by the loss of drift (the rain-out). As in region II, the in-situ formation of dust grains is impossible. The grains reach their maximum radius in this region III: $\langle a \rangle \approx 0.3\,\mu$m , $2\,\mu$m , $20\,\mu$m , $100\,\mu$m for $\tau_{\rm mix} = 10^6$s , 10^5s , 10^4s , 10^3s , respectively, at moderate drift velocities, e. g. $\langle \vec{v}_{\rm dr} \rangle \approx 15\,$cm/s for $\tau_{\rm mix} = 10^4$s. However, since the residence time-scale of the sinking grains is limited, the particles do not grow significantly in the nearly saturated gas: $\langle a \rangle$ increases slower than in region II.

IV. Evaporating grains: The gravitationally settling dust particles finally cross the cloud base and sink into the undersaturated gas situated below, where $S < 1$ and $\chi_{\rm lKn}^{\rm net} < 0$. The evaporation of these dust particles, however, does not take place instantaneously which results in a spatial extension of region IV of about 100 m in our $T_{\rm eff} = 1400\,$K models. Region IV is hence characterised by drift $\leftrightarrow$ evaporation, i. e. the dust grains, which are raining in from above, evaporate thermally. The release of condensable matter from the surface of the evaporating grains in fact *enriches* the gas below the cloud base with heavy elements $\epsilon_{\rm gas}^{\rm Ti} > \epsilon_{\rm Ti}^{0}$. This enrichment, in return, tends to saturate the gas $S \lesssim 1$. With decreasing altitude the particles get smaller $d\langle a \rangle / dz < 0$ and slower $d\langle v_{\rm dr} \rangle / dz < 0$. Consequently, their residence times increase, and a run-away process results in a sharp lower edge of the cloud, given by the point where even the largest particles have evaporated completely. We note that region IV, in particular, cannot be understood by stability arguments, but requires a treatment of the dust complex by means of differential equations.

3.2 Influence of mixing

The sequence of Figs. 2 to 3 demonstrates the influence of the convective mixing on the calculated cloud structures and dust particle properties. With increasing strength of the convective mixing (decreasing $\tau_{\rm mix}$)

1) the ϵ-gradient of the remaining condensable elements in gas phase of the atmosphere becomes shallower (the upper atmosphere becomes less depleted and the gas below the cloud base becomes less enriched for strong mixing),

2) the positions and spatial extensions of regions I, II and III are changing, in particular region I (significant $J_\star$) is extended and region III ($S \gtrsim 1$) disappears for strong mixing, and

3) the dust particles and their mean drift velocities become larger.

Without mixing, the atmosphere would become throughout saturated, i. e. a very steep ϵ-gradient would establish, according to the exponential temperature-dependency of the supersaturation ratio S (see Eq.13). Strong mixing counteracts this effect and washes out this gradient, which explains point 1.

According to point 1, strong mixing leads to a less metal-deficient upper atmosphere, which produces a more active and more extended nucleation zone I. Concerning region III, the characteristic self-regulation mechanism $S \rightarrow 1$ requires that growth is more efficient than mixing. For too vivid mixing, this case cannot be reached and region III disappears, which explains point 2.

A faster replenishment of the atmosphere with condensable elements via strong mixing also leads to a higher concentration of these elements in region II, which is mainly responsible for the growth of the particles. Consequently, more matter condenses on the surface of the dust particles during their descent through the atmosphere, resulting in larger particles with larger drift velocities, which explains point 3.

3.3 Influence of effective temperature

Figure 4 depict two model calculations for a lower effective temperature $T_{\rm eff} = 1000\,{\rm K}$. Only the two extreme cases ($\tau_{\rm mix} = 10^6\,{\rm s}$ and $\tau_{\rm mix} = 10^3\,{\rm s}$) are shown. In general, the resulting cloud structures are similar to those obtained for the $T_{\rm eff} = 1400\,{\rm K}$-model, but their location is different. For lower $T_{\rm eff}$, the active dust formation regions are situated deeper inside (note the different scaling of the x-axis) and the gas in the observable layers above the $\tau_{\rm R} = 1$ level becomes more metal-deficient. The latter result, an increasingly metal-poor gas for lower $T_{\rm eff}$, has been suggested as explanation for the disappearance of certain molecular features (like TiO and FeH) in the observed spectra of L dwarfs in comparison to M dwarfs (e. g. Leggett et al. 2001). According to the larger densities in the active dust formation regions of the $T_{\rm eff} = 1000$K-model, the particles also become slightly larger as compared to the $T_{\rm eff} = 1400$K-model.

3.4 The dust-to-gas ratio above the cloud base

All depicted models are featured by an almost constant dust-to-gas ratio well above the cloud base (see $\epsilon_{\rm dust}$ in Figs. 2, 3 and 4), approximately equal to the mass fraction of condensable elements in the gas being mixed up (here $\epsilon^0_{\rm Ti}$). This is a natural result of an undisturbed, complete condensation process. Evidently, the disturbance of the dust formation process by rain-out and mixing is small in our models, in agreement with the time-scale discussion of Paper II, where it was shown that the drift motion of dust grains in brown dwarf atmospheres usually operates on much longer time-scales than nucleation and growth.

However, if the elemental replenishment by convective mixing becomes too ineffective, the maximum dust-to-gas ratio present in the atmosphere starts to deviate from $\epsilon^0_{\rm Ti}$ and finally vanishes as shown in Fig. 5. In this case, the loss of

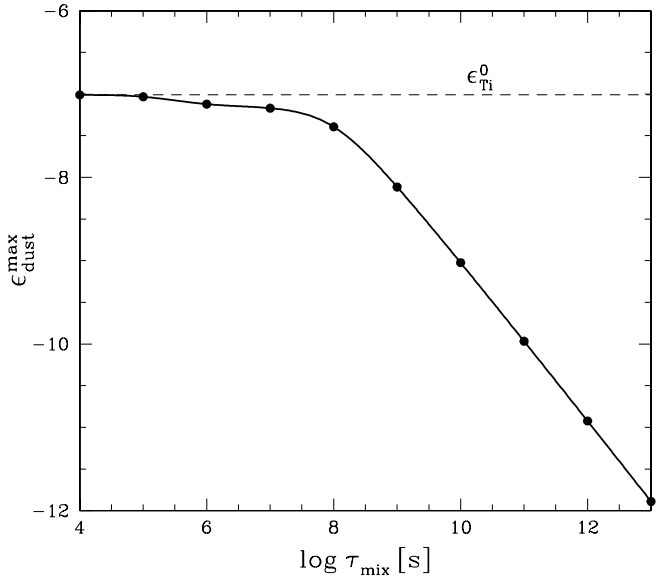

Abbildung 5: Maximum of the dust-to-gas ratio expressed in terms of $\epsilon^{\rm max}_{\rm dust} = \max_z\{\rho(z)L_3(z)/(n_{\langle \rm H\rangle}(z)\Delta V_{\rm TiO_2})\}$ as function of the mixing time-scale $\tau_{\rm mix}$. The circles indicate the calculated models for $T_{\rm eff} = 1400\,$K. In comparison, the solar titanium abundance $\epsilon^0_{\rm Ti}$ is shown as dashed line.

condensable elements from a gas with maximum dust-to-gas ratio via rain-out, even if the dust particles are very small, is larger than the gain of condensable elements by mixing. Consequently, the actual dust-to-gas ratio above the cloud base is limited by the mixing in this case and finally scales as $\epsilon^{\rm max}_{\rm dust} \propto 1/\tau_{\rm mix}$. For $\tau_{\rm mix} \rightarrow \infty$, the gas becomes completely dust-free, in agreement with the mathematical discussion in Appendix A.

We conclude that the upper atmospheric layers of brown dwarfs should be dusty as long as the convective mixing time-scale $\tau_{\rm mix}$ is shorter than about $10^8\,$s $\approx 3\,$years, since enough condensable material is continuously mixed up by the convection in this case. This value might provide a reasonable criterion for the definition of a "cloud deck" in the convective $\rightarrow$ radiative transition region of brown dwarf atmospheres, where $\tau_{\rm mix}$ is expected to increase strongly[7].

Noteworthy, the dust-to-gas mass ratio $\propto \epsilon_{\rm dust}$ also starts to deviate from $\epsilon^0_{\rm Ti}$ shortly above the cloud base in case of strong mixing (see $\tau_{\rm mix} = 10^3\,$s-models on the r.h.s. of Figs. 3 and 4). The dust grains and their drift velocities become so large in this case that a considerable loss by rain-out sets in. The result is a lowering of the dust-to-gas ratio shortly above the cloud base. Additionally, the competing process (the growth) is handicapped here, because the total surface area of the dust component is small in case of a few large grains as compared to many small grains. In fact, this is the main reason why the supersaturation ratio S already deviates from unity above the cloud base in the $\tau_{\rm mix} = 10^3\,$s-models.

[7]See also the discussion in Sect. 4.2.

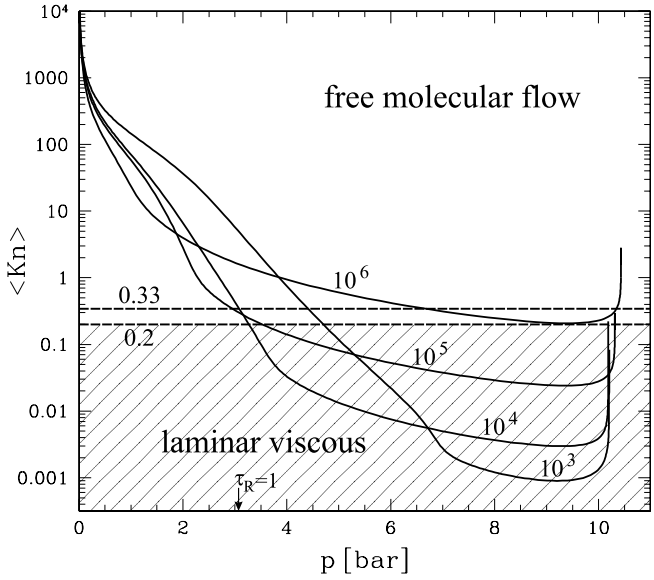

Abbildung 6: Mean Knudsen number of the dust component, derived from $\langle a \rangle$, as function of the gas pressure for the $T_{\rm eff} = 1400\,$K-models. The labels mark the assumed value for $\tau_{\rm mix}\,[{\rm s}]$. The dashed lines indicate the critical Knudsen numbers for friction and growth, respectively (compare Paper II).

4 Discussion and outlook

4.1 Validity of the $\mathrm{Kn} \gg 1$ approximation

In this paper, we have focused on the $\mathrm{Kn} \gg 1$ case, which enabled us to use an unique system of dust moment equations throughout the atmosphere[8]. However, Fig. 6 shows that the Knudsen numbers may fall short of unity in the deeper layers, for example below $p \approx (3 \ldots 5)\,$bar in the $T_{\rm eff} = 1400\,$K-models. This means that the mean free path of a gas particle becomes smaller than a typical grain diameter. The physical description for the growth and the frictional force are different in this case, i. e. our model can only provide a possibly quite rough picture from these layers. Here, the true drift velocities are probably larger and the true growth velocities are probably smaller as compared to our results, i. e. we expect that the dust particles remain smaller in the deeper layers as compared to Figs. 2, 3 and 4.

Figure 6 also demonstrates that the outer regions can very well be treated in the $\mathrm{Kn} \gg 1$ limiting case. Since the problem is formulated in terms of first order differential equations which are integrated inward, the solution in the outer regions does not depend on the uncertainties concerning the deeper layers. Therefore, we conclude that our results are appropriate for the upper layers, approximately down to the $\tau_{\rm R} = 1$ level, which are most interesting from an observational point of view. The results are also OK for not too vivid mixing, e. g. for $\tau_{\rm mix} \gtrsim 10^6\,$s in Fig. 6.

[8] A different system of dust moment equations for the opposite case $\mathrm{Kn} \ll 1$ has been derived in Paper II.

A more realistic description of the deeper layers could be achieved by performing a Knudsen number fall differentiation with respect to $\langle \mathrm{Kn} \rangle$, i. e. to start with the $\mathrm{Kn} \gg 1$ moment equations in the outer layers as outlined in this paper, but then to switch to the $\mathrm{Kn} \ll 1$ moment equations (see Paper II) as soon as $\langle \mathrm{Kn} \rangle$ has dropped below a certain critical value, e. g. 0.3. However, such a procedure is problematic anyway, since all dust particles in the size distribution function would be treated in the same Knudsen number limiting case. A more profound solution would require the integration over the size distribution, which could approximately be determined from the calculated dust moments (see Sect. 6.5 in Paper II).

4.2 Convective mixing

The results presented in Sect. 3 have been obtained by assuming a stationary replenishment of the whole atmosphere with dust-free gas of solar abundances (from the deep interior of the brown dwarf) on a constant, depth-independent time-scale τ_{mix}. Although this approach is certainly a poor description of the true convective mixing occurring in these atmospheres, it has allowed for a first detailed study of the cloud structures in brown dwarf atmospheres, simple enough to investigate the influence of the mixing on the dust formation in a systematic way. There are, however, also some uncertainties introduced by this approach.

- The effect of convective mixing is obviously depth-dependent. In particular, the upper atmosphere will become purely radiative at some point, i. e. truly static (quiescent) and mixing-free. As argued in Sect. 2.2, such layers must become saturated and completely dust-free for $t \rightarrow \infty$, because the system has infinite time to relax toward phase equilibrium ($S = 1$) and even the smallest dust particles will settle gravitationally[9]. Therefore, the dust-to-gas mass ratio ($\propto L_3$) cannot remain constant (as resultant from our current model) for $\tau_{\mathrm{mix}} \rightarrow \infty$, which probably occurs for $z \rightarrow \infty$. Thus, we expect that the outer edge of the convective zone provides a natural borderline for the cloud layers (cloud decks).

- Considering a convectively ascending bubble of gas from the deep interior, which is dust-free at first, the temperature / density conditions will change gradually in this element, meaning that the key process of nucleation and the dust growth can already occur during the ascent of this element, i. e. well before the element has reached the upper atmospheric layers where it finally disperses in the surrounding gas. Furthermore, turbulent small-scale temperature-fluctuations may result in considerable nucleation rates even at high temperatures (see Helling et al. 2001, henceforth called Paper I, and Sect. 4.3). Consequently, the nucleation can be expected to occur already in lower, warmer regions on the average (as sketched in Fig. 1) and our nucleation region I could be an artifact of our very strongly simplified approach for the convective mixing.

[9]Sometimes, there are two or more convective layers according to models of brown dwarf atmospheres (e. g. Tsuji 2002). The above argumentation can be extended to such secondary convective layers if they are convectively disconnected from the large reservoir of uncondensed matter in the deep interior of the brown dwarf or, at least, if the convective layer does not reach deep enough to contain the evaporation zone IV.

The first point could be accounted for by using a depth-dependent approach for $\tau_{\rm mix}$ in future models, e. g. $\tau_{\rm mix}(z) = \alpha_{\rm mix} H_p / \bar{v}_{\rm conv}(z)$ where the mean convective velocity $\bar{v}_{\rm conv}(z)$ could be adopted from a convection model, e. g. from mixing length theory. Performing 3D convection simulations for M dwarfs, Ludwig et al. (2002) have noted that a convective zone does not end abruptly, but that an exponential ansatz for $\bar{v}_{\rm conv}(z)$ around the convective $\rightarrow$ radiative transition zone is more realistic. In return, the dust formation may also have an important influence on the convection, e. g. via the release of the heat of condensation during the grain growth process or via opacity effects. For example, Helling et al. (2001) have shown that the increase of the opacity due to dust formation will effect a transition from an almost adiabatic $\rightarrow$ an almost isothermal behaviour of the dust/gas mixture. Thus, a consistent treatment of convection and dust formation is required to come to more definite conclusions.

The second point could be improved by using a diffusive approach for the mixing. Investigating the burning and the convective mixing of deuterium in pre-main sequence stars, Wuchterl & Tscharnuter (2003) have proposed to quantify the local net gain of species k by convective mixing via $-\nabla \vec{j}_k^{\rm conv}$ where the mean convective flux of species k is given by

$$\vec{j}_k^{\rm conv} = - \frac{\alpha_{\rm ML} H_p}{2} \, \bar{v}_{\rm conv} \, \rho \nabla c_k \ . \tag{14}$$

$\alpha_{\rm ML} \approx 1.5$ is the mixing length parameter and c_k the mass concentration of species k. Adopting this approach to our problem, the mixing term $-\nabla \vec{j}_k^{\rm conv}$ with $c_k = \{L_j, \epsilon_i\}$ could be used instead of $-\rho L_j / \tau_{\rm mix}$ and $n_{\langle \rm H \rangle} (\epsilon_i^0 - \epsilon_i) / \tau_{\rm mix}$ in Eqs. (5) and (6), respectively. In that case, the equation system to be solved becomes a system of second order partial differential equations with the need to specify inner and outer boundary conditions, a problem which requires a more careful numerical treatment. We note, however, that the character of the convective mixing can, at least partly, also be large-scale, i. e. it is possible that an uncondensed bubble of gas from the interior reaches the upper layers and disperses before it cools and condenses, where our simple ansatz with $\tau_{\rm mix}$ seems appropriate.

However, these one-dimensional approaches for the convection, considering temporal and spatial averages, can only provide a rough description of the underlying hydrodynamical processes. A more direct approach was a 3D dynamical simulation, where a description of the large-scale mixing becomes obsolete. We want to emphasise, however, that even in such models (e. g. LARGE EDDY SIMULATIONS) the true mixing down to the Kolmogoroff-scale requires a sub-grid modelling, because the smaller scales cannot be resolved on the typically large-scale computational grids (see e. g. Menevean & Katz 2000, Pijpers & Habing 1989). Furthermore, structure formation processes are often seeded in the small scale regime, as known e. g. from combustion engineering.

4.3 Comparison to other models

According to our present knowledge, we have presented the first model calculations for brown dwarf atmospheres where the coupled problem of dust formation, precipitation and element consumption has been solved on the basis of a kinetic description of the underlying physical and chemical processes. A consistent

incorporation of this description into classical stellar atmosphere models (to account for the important feedbacks of the dust on the atmospheric structure via radiative transfer effects and the convection) has not yet been achieved.

So far, other works have mainly focused on the consequences of the dust formation on the spectral appearance of brown dwarfs, thereby treating the dust complex in a much more simplified way. These approaches have in common that the possible existence and the properties of the dust particles are completely deduced from *local* arguments and considerations. A possible connection between the site of formation (nucleation) of a dust grain and its occurrence in another place (via winds or gravitational settling) has not been considered in any other model.

Allard et al. **(2001)** have relied on the assumption of chemical and phase equilibrium between the molecules in the gas and a huge collection of solid and liquid materials. If a solid material is found to be thermodynamically stable, the respective elements are depleted from the gas phase down to the $S=1$-level and the amount of dust present in the atmosphere is either given by element conservation constraints (the case of complete condensation) or is assumed to be zero (the case of complete gravitational settling). Each condensate is assumed to be present in form of homogeneous spherical particles, i. e. no dirty or core-mantle grains. The size distribution known from the interstellar medium is utilised.

According to our model, phase equilibrium ($S=1$) is only valid at the cloud base. All other regions are out of phase equilibrium because of incomplete growth or evaporation. However, the self-regulation mechanism characteristic for our region III (see Sect. 3.1) approximately installs $S\approx 1$ in a considerably extended layer around the cloud base. Thus, the assumption of phase equilibrium is in fact reasonable in certain parts of the atmosphere. The thickness and the location of this zone depends on the condensate and, in particular, on the strength of the convective mixing. For too vivid mixing, this zone disappears.

Tsuji (2002) has suggested that condensates in cool dwarf atmospheres are present in form of layers with strict inner and outer boundaries. The inner boundary, associated with a certain temperature denoted by $T_{\rm cond}$, is related to the thermodynamical stability of the dust material in the surrounding gas of solar abundances. The upper boundary, parameterised by $T_{\rm cr}$, is related to the assumption, that the dust particles must remain extremely small (of the order of the critical cluster size $r_{\rm cr}$), because they would grow too large and start to settle gravitationally otherwise. For $T_{\rm cond} > T > T_{\rm cr}$, the particles are assumed to be constantly forming and re-evaporating, thereby circumventing the problem of the gravitational settling.

Our results suggest that the loss of condensable matter via dust formation and precipitation in the atmosphere can easily be balanced by the elemental replenishment via convective mixing. Therefore, we think that there is no need to circumvent the precipitation. An ongoing process of nucleation $\rightarrow$ growth $\rightarrow$ precipitation $\rightarrow$ evaporation $\rightarrow$ mixing can be maintained as long as convection is active. We also disagree with the upper chemical argumentation, because the critical cluster corresponds to an *unstable* equilibrium (the critical cluster is the most unstable cluster on the most efficient chemical pathway to dust, see

e. g. Feder et al. 1966). It will be difficult to maintain a system like a brown dwarf atmosphere in such a fine-tuned unstable equilibrium state. According to our model, the upper atmospheric regions can in fact contain a large amount of very small dust particles, but the formation of these particles is a kinetic consequence of the effective nucleation rates and cannot be explained by stability considerations.

On open question is whether the dust can indeed only exist in convective layers. Takashi Tsuji (priv. com.) notes that in his models of warm L dwarfs, the convective zone start too deep to interact with the cloud layers, which are situated higher. We remark, however, that already a very small mixing activity ($\tau_{\rm mix} \lesssim 10^8\,{\rm s}$) is enough to make the atmosphere dusty (see Sect. 3.4) and that mixing length theory may be too rough to quantify the exponentially increasing mixing time-scale above the convective $\rightarrow$ radiative transition zone (Ludwig et al. 2002). Concerning the Earth's atmosphere, the approximately adiabatically stratified troposphere is just the place where circulation occurs and water condenses. In contrast, the stratosphere, as transition region to the radiative mesosphere, is quiescent and usually free of water droplets, so there seems to exist a close correlation between condensation and convection at least in the case of the Earth's atmosphere.

Cooper et al. **(2003)** utilise the chemical and phase equilibrium code of Burrows & Sharp (1999) to determine whether dust particles of a certain kind are thermodynamically stable in a solar composition gas. If stability is assured, the mean size of the particles is deduced from local time-scale arguments based on Rossow (1978), considering growth, coagulation (also termed as coalescence), precipitation and convective mixing. The amount of dust is prescribed by introducing a free parameter $S_{\rm max} \approx 0.01$, denoted by the maximum supersaturation. Thereby, the supersaturation ratio of the gas (denoted by S in our paper) is fixed throughout the atmosphere and the mass of dust present in the atmosphere scales with the saturation vapour pressure $p_{\rm sat}(T)$, which decreases exponentially with decreasing temperature. Consequently, the vertical structure of the dust is a layer with a strict lower boundary and an exponentially decreasing dust-to-gas ratio above the cloud base.

It is interesting to note that Cooper et al. (2003) derive similar particle sizes ($5\,\mu{\rm m} \ldots 300\,\mu{\rm m}$) as compared to our model, although the physical description, e. g. of the dust growth, is very different. We find, however, that the mean size of the dust particles $\langle a \rangle$ is usually much smaller than the maximum particle size $a_{\rm max}$ as derived from local time-scale arguments (see Paper II), in particular regarding the upper atmospheric layers. Thus, local time-scale arguments are not sufficient, but the problem requires a kinetic treatment. We furthermore remark that, in contrast to Cooper et al. (2003), our results suggest that the supersaturation ratio S varies strongly with altitude, in particular regarding higher atmospheric layers. The supersaturation ratio S is also strongly affected by the convective mixing.

In the Cooper et al. model, the mean particle size is a function of depth and condensate. The largest particles are located at the cloud base, which is in agreement with our results. This might be of observational relevance since the degree of polarisation increases strongly with increasing particle size and multiple scattering can even amplify this effect (Sengupta & Krishan 2001). Po-

larisation measurements may therefore open up a possibility to deduce the mean size of the dust particles around the cloud bases in brown dwarf atmospheres. According to Sengupta (2003), the observed polarisation of the brown dwarf DENIS-P J0255-4700 ($T_{\rm eff} \approx 1400\,{\rm K}$, $\log\, g \approx 5$) can be explained by a maximum grain radius of about $5\,\mu$m, if single scattering of spherical particles is considered. This lies well in the range of maximum sizes derived from our models and could represent the case $\tau_{\rm mix} \approx 10^5\,{\rm s}$ (see r.h.s. of Fig. 2).

Helling et al. **(2001)** have studied the onset of the dust formation process in small ascending convective gas elements under turbulent conditions typical for brown dwarf atmospheres. The same physical description of nucleation and dust growth is applied as in this paper, except for the evaporation and the particle drift which have been neglected. The convection is assumed to energise turbulence, which creates a strongly varying velocity field and fluctuations of all thermodynamical quantities on various length scales, down to the Kolmogoroff-scale ($\eta \approx 10^{-2}\,{\rm cm}$). Acoustic waves are shown to be capable to initiate the dust formation process via nucleation events caused by the superposition of two or more expansion waves, even in layers which are usually too hot for nucleation. The refractory elements in the gas phase soon condense on the surface of these first seed particles. When a considerable fraction of the condensable elements is consumed, the increasing dust opacity reinforces radiative cooling and causes the thermodynamical behaviour of the gas-dust-mixture to change from almost adiabatic to almost isothermal (fast radiative relaxation), which in return might affect the convective stability of the atmosphere. The dust component results to be spatially very inhomogeneous.

We want to clarify that the effect of *turbulent small-scale fluctuations* on the dust formation has been neglected in the current paper – although it may be important. The aim of this paper is to understand the *large-scale structure* of a cloud layer in brown dwarf atmospheres. Accordingly, we have developed a model for the largest scales where the small-scale processes can principally not be resolved. In order to include such effects approximately, appropriate sub-grid closure terms for the dust moment equations must be developed.

5 Conclusions

In this paper, first model calculations for cloud layers in static brown dwarf atmospheres have been presented which are based on a kinetic description of the underlying microphysical and chemical processes nucleation, growth, evaporation, element depletion, sedimentation and mixing. We have used a system of differential equations for the moments of the dust size distribution function, which has been developed in Paper II, in the stationary case for large Knudsen numbers. The consumption of condensable elements is an essential part of this description and, therefore, the depletion of the gas phase from condensable elements is a consistent part of the results. The model calculations are restricted to one exemplary refractory dust species, TiO_2, which is enough to study the control mechanisms for the dust formation and the general structure of cloud layers in brown dwarf atmospheres.

According to our results, an ongoing cycle of nucleation $\rightarrow$ growth $\rightarrow$ precipitation $\rightarrow$ evaporation characterises the large-scale structure of a cloud layer,

related to the life cycle of dust grains in brown dwarf atmospheres. This cycle is driven by the convection. Without convection, all dust particles would settle gravitationally, leaving behind a saturated (i. e. strongly metal-deficient) dust-free atmosphere above the cloud base. However, cool dwarf stars (M, L, T) are almost fully convective, which leads to a replenishment of the upper atmosphere with condensable elements from the deep interior of the star. Thus, the convection triggers the formation and resultant properties of the emergent dust particles.

Four distinct regions can be distinguished, ordered by the leading physical process for the dust component which corresponds to a particular height above a cloud base in a quasi-static model[10]:

1) *Nucleation:* The formation of seed particles occurs high in the atmosphere (e. g. $T < 1300\,\mathrm{K}$ to $T < 1500\,\mathrm{K}$ for TiO_2, depending on the mixing) where the gas is highly supersaturated[11], but nevertheless strongly depleted (metal-poor).

2) *Growth:* These particles slowly sink into lower regions, where the in-situ formation (nucleation) becomes impossible. The particles grow substantially in these layers, thereby consuming the condensable elements which are constantly replenished by the convective mixing. The growth process remains incomplete in these layers, i. e. the gas remains highly supersaturated.

3) *Drift:* With increasing density in the deeper layers, the growth process becomes complete, which results in an almost saturated gas. The dust particles mainly drift through this region without much further growth.

4) *Evaporation:* The dust particles finally cross the cloud base (defined by $S = 1$, here at $T \approx 2000\,\mathrm{K}$ for TiO_2) and populate the undersaturated gas below. The evaporation of these dust particles creates a metal-enriched region and shifts the borderline of the physical existence of dust particles well below the cloud base.

This stratification cannot be understood by stability arguments, but requires a kinetic treatment of the dust complex. According to our results, the atmosphere is generally in phase-non-equilibrium ($S \neq 1$), except for the cloud base, where the element abundances coincide with those of the uncondensed gas which is mixed up. Consequently, the application of numerical codes which assume chemical and phase equilibrium, simply including liquid and solid phases as additional specimen, seems questionable. However, a self-regulation mechanism exists for not too vivid mixing which leads to the formation of a restricted layer around the cloud base where phase equilibrium is approximately valid ($S \approx 1$).

[10] In time-dependent simulations (e. g. Paper I), this classification corresponds rather to different *phase* of the dust formation process than to a particular height in the atmosphere.

[11] It is important to note that the formation of high-temperature condensates (with sublimation temperatures of the order of 2000 K) requires to overcome the nucleation barrier. The pre-existence of some seed particles in the condensing gas of another unidentified kind (in analogy to the aerosols in the Earth atmosphere) seems questionable here, because the temperature difference nucleation-stability (here 500 K to 700 K) is large compared to the difference of the sublimation temperatures between TiO_2 and other candidates of high-temperature condensates.

The location and spatial extension of this layer depends on the material, the stellar parameters and the convective mixing.

From an observational point of view, it is important to note that the gas becomes more and more depleted in the upper atmosphere. The maximum degree of depletion of Ti with respect to the cloud base results to be 3.5 to 6.5 orders of magnitude in our model, depending on the efficiency of the convective mixing. These layers are mainly responsible for the observational molecular features.

Beside the element abundances in the gas phase and the supersaturation ratio, the model makes predictions about the large-scale dust structure of a cloud layer, in particular the dust-to-gas mass ratio and the mean size of the dust particles present in the atmosphere. The overall cloud structure is characterised by an almost constant dust-to-gas ratio for constant mixing above the cloud base and a sudden drop at the lower physical borderline, where the dust particles shrink, decelerate and vanish. The mean particle size $\langle a \rangle$ is generally found to decrease by several orders of magnitude from a maximum value present at the cloud base with increasing height. Depending on the convective mixing, this maximum size ranges in $0.3\,\mu$m to $150\,\mu$m, which is consistent with the quantity $a_{\max}$ defined in Paper II. However, the particles generally remain much smaller than $a_{\max}$ high above the cloud base and/or in case of weak convective mixing.

A lower effective temperature $T_{\rm eff}$ of the brown dwarf mainly results in a shift of the active dust formation zone into deeper layers, finally below the observable limit $\tau_{\rm R} \approx 1$. The general structure of the cloud layer and the resultant properties of the dust particles remain similar with respect to the cloud base. However, if only the results at $\tau_{\rm R} = 1$ are considered, the dust particles are smaller (but more numerous) and the gas phase is more depleted for lower $T_{\rm eff}$.

In general, a more reliable treatment of the dust complex in the atmospheres of cool dwarfs and giant gas planets can be obtained by a quantitative description of nucleation, net growth, element depletion and sedimentation of the dust particles by means of differential equations. *Local arguments and considerations*, which have been mainly used so far, *are not sufficient* because they cannot account for the fact that dust particles can be created in one place and can occur in another place, which leads to a spatial (and temporal) coupling of the problem.

Beside an extension of our preliminary models to more than one dust species (which involves the problem of core-mantle and possibly dirty grains), the development of turbulent closure terms for small-scale fluctuations and a more general treatment of small and large Knudsen numbers, the remaining uncertainties of our current model are mainly introduced by our strongly simplified treatment of the convective mixing. A fine-tuned equilibrium between the *upward directed flux of condensable elements via convection* and the *downward transport of condensable elements via the formation, gravitational settling and thermal evaporation of dust grains* is responsible for the vertical structure of the condensable elements. In particular, the decreasing efficiency of the convective mixing around the convective $\rightarrow$ radiative transition zone seems important to understand the cloud decks. Moreover, since the dust formation may even have an important feedback on the convection itself (via the release of the latent heat of condensation and via opacity effects), a simultaneous treatment of convection and dust formation, consistently coupled to a frequency-dependent radiative transfer, is required for more realistic models of brown dwarf atmospheres.

Acknowledgement: We thank Takashi Tsuji for providing us with exemplary brown dwarf model structures. This work has been supported by the *DFG* (grand SE 420/19-1, 19-2 and Sonderforschungsbereich 555, part project B8). Most of the literature search has been performed with the ADS system.

A The static solution without mixing

In order to discuss the possible existence of dust particles in a truly static atmosphere, we consider the dust moment and element consumption equations without mixing (Eqs. 1 and 4) in the static stationary case, where all l.h.s. terms vanish. Concerning Eq. (4), both source terms on the r.h.s. are negative in case of supersaturation and positive in case of undersaturation[12]. Since their sum is zero in the static case, each term must be zero, i. e.

$$J(V_\ell) = 0 \quad \text{and} \quad \{S = 1 \ \text{ or } \ L_2 = 0\} \ . \tag{15}$$

From the definition of the dust moments as integrals over a strictly positive size distribution function $f(V) \geq 0$, multiplied by some power of the positive volume $V^j \geq 0$, it is clear that $L_2 = 0$ implies $L_j = 0$ for all j. Furthermore, $S = 1$ implies that $\chi^{\rm net}_{\rm lKn} = 0$ according to Eq. (2). Consequently, Eq. (15) is equivalent to

$$J(V_\ell) = 0 \quad \text{and} \quad \left\{\chi^{\rm net}_{\rm lKn} = 0 \ \text{ or } \ L_j = 0\right\} \ . \tag{16}$$

Thus, the following conclusions can be drawn:

$S<1$: According to Eq. (2), undersaturation implies $\chi^{\rm net}_{\rm lKn} < 0$. We can hence conclude from Eq. (16) that the gas must be dust-free $L_j = 0$. This is the usual case of "normal" stellar atmospheres, where the gas is too hot for saturation and all dust particles have disappeared (if ever existed) due to evaporation.

$S=1$: Saturation implies $\chi^{\rm net}_{\rm lKn} = 0$ according to Eq. (2). Inserting this result into the dust moment equations (Eq. 1), we can deduce that $\frac{d}{dz}(dL_j/c_T) = 0$ for all j or

$$L_j = {\rm const}_j \cdot c_T = {\rm const}_j \cdot \sqrt{2kT/\bar{\mu}} \ . \tag{17}$$

This solution describes the pure effect of drift on the dust moments, i. e. dust particles which drift through the atmosphere without changing their properties. However, at some depth in the atmosphere the gas must become undersaturated because of the inward increasing temperature. A continuous transition to the $S<1$ case is hence only possible if ${\rm const}_j = 0$ for all j. Physically speaking, the dust particles cannot simply disappear at the borderline to $S<1$, but have to evaporate there which would constantly enrich this layer with condensable elements – in contradiction to the assumption of a static atmosphere. We conclude that the gas must be dust-free also for $S=1$.

[12] As argued in Paper II, $S_r = S^{m_r}$ is valid for simple types of growth reactions, where m_r denotes the number of monomers of the solid compound created by that reaction. Therefore, e. g. $S>1$ is equivalent to $S_r>1$ for all r.

$S > 1$: This case contradicts the $J(V_\ell) = 0$ condition, because supersaturation always implies a possibly very small but in any case non-vanishing nucleation rate.

Consequently, the gas cannot be supersaturated ($S \leq 1$) and must be dust-free ($L_j = 0$) in a truly static atmosphere. This solution is denoted by the "trivial solution" in Sect. 2.2.

Literatur

Ackermann S., Marley M., 2001, ApJ 556, 872–884

Allard F., Hauschildt P., Alexander D., Tamanai A., Schweitzer A., 2001, ApJ 556, 357–372

Burgasser A., Marley M., Ackerman A., Saumon D., Lodders K., Dahn C., Harris H., Kirkpatrick J., 2002, ApJ 571, L151–L154

Burrows A., Sharp C. M., 1999, ApJ 512, 843–863

Chabrier G., Baraffe I., 1997, A&A 327, 1039–1053

Chase Jr. M. W., Davies C. A., Downey Jr. J. R., Frurip D. J., McDonald R. A., Syverud A. N., 1985, *JANAF Thermochemical Tables*, National Bureau of Standards

Cooper C. S., Sudarsky D., Milsom J. A., Lunine J. I., Burrows A., 2003, ApJ submitted

Deuflhard P., Wulkow M., 1989, IMPACT Comp. Sci. Eng. 1, 269–301

Dominik C., Sedlmayr E., Gail H.-P., 1993, A&A 277, 578–594

Feder J., Russell K. C., Lothe J., Pound G. M., 1966, Adv. Phys. 15, 111–178

Gail H.-P., Sedlmayr E., 1988, A&A 206, 153–168

Gail H.-P., Keller R., Sedlmayr E., 1984, A&A 133, 320–332

Gauger A., Gail H.-P., Sedlmayr E., 1990, A&A 235, 345–361

Gelino C. R., Marley M. S., 2000, In Griffith C. A., Marley M. S., *From Giant Planets to Cool Stars*, 322–330

Gierasch P., Ingersoll A., Banfiled D., Ewald S., Helfenstein P., Simon-Miller A., Vasavada A., Breneman H., Senske D., the Galileo Imaging Team, 2000, Nature 403, 628–629

Hairer E., Wanner G., 1991, *Solving Ordinary Differential Equations II*, Springer, Berlin

Helling Ch., Winters J. M., Sedlmayr E., 2000, A&A 358, 651–664

Helling Ch., Oevermann M., Lüttke M., Klein R., Sedlmayr E., 2001, A&A 376, 194–212 (Paper I)

Kirkpatrick J. D., Reid I. N., Liebert J., Cutri R. M., Nelson B., Beichman C. A., Dahn C. C., Monet D. G., Gizis J. E., Skrutskie M. F., 1999, ApJ 519, 802–833

Leggett S. K., Allard F., Geballe T. R., Hauschildt P. H., Schweitzer A., 2001, ApJ 548, 908–1018

Ludwig H.-G., Allard F., Hauschildt P. H., 2002, A&A 395, 99–115

Lunine J. I., Hubbard W. B., Burrows A., Wang Y.-P., Garlow K., 1989, ApJ 338, 314–337

Marley M., Seager S., Saumon D., Lodders K., Ackerman A., Freedman R., Fan X., 2002, ApJ 568(1), 335–342

Meneveau C., Katz J., 2000, Annu. Rev. Fluid Mech. 32, 1–32

Patzer A. B. C., Chang C., Sedlmayr E., Sülzle D., 1999, Eur. Phys. J. D 6, 57–62
Pijpers F. P., Habing H. J., 1989, A&A 215, 334–346
Rossow W. V., 1978, Icarus 36, 1–36
Sengupta S., 2003, ApJL 585, L155–L158
Sengupta S., Krishan V., 2001, ApJL 561, L123–L126
Tsuji T., 2002, ApJ 575, 264–290
Vasavada A., Ingersoll A., Banfield D., Bell M., Gierasch P., Belton M., Orton G., Klaasen K., DeJong E., Breneman H., Jones T., Kaufmann J., Magee K., Senske D., 1998, Icarus 135, 265–275
Woitke P., Helling Ch., 2003, A&A 399, 297–313, (Paper II)
Wuchterl G., Tscharnuter W. M., 2003, A&A 398, 1081–1090
Wulkow M., 1992, IMPACT Comp. Sci. Eng. 4, 153–193